Effects of calcination conditions on phase and morphology evolution of lead zirconate powders synthesized by solid-state reaction

W. Chaisan · O. Khamman · R. Yimnirun ·
S. Ananta

Abstract Lead zirconate ($PbZrO_3$) powder has been synthesized by a solid-state reaction via a rapid vibro-milling technique. The effects of calcination temperature, dwell time and heating/cooling rates on phase formation, morphology, particle size and chemical composition of the powders have been investigated by TG-DTA, XRD, SEM and EDX techniques. The results indicated that at calcination temperature lower than 800 °C minor phases of unreacted PbO and ZrO_2 were found to form together with the perovskite $PbZrO_3$ phase. However, single-phase $PbZrO_3$ powders were successfully obtained at calcination conditions of 800 °C for 3 h or 850 °C for 1 h, with heating/cooling rates of 20 °C/min. Higher temperatures and longer dwell times clearly favored the particle growth and formation of large and hard agglomerates.

Introduction

Lead zirconate, $PbZrO_3$ (PZ), which is a typical antiferroelectric (AFE) material at room temperature with a Curie temperature of ~230 °C, has an orthorhombic symmetry with a structure similar to that of classical ferroelectric of orthorhombic barium titanate (BaTiO_3) [1–5]. Practically, this material is a potential candidate for energy storage applications for DC fields and low loss linear capacitor, owing to its AFE nature [6–12]. Recently, the double hysteresis behavior of this material makes it attractive for the microelectronic, microelectromechanical systems (MEMs) as well as for actuator applications [12–14].

Lead zirconate when combined with other oxides can form a series of solid solution materials such as $Pb(Zr_x,Ti_{1-x})O_3$, $PbZrO_3$–$Pb(Mg_{1/3}Nb_{2/3})O_3$, $PbZrO_3$–$PbTiO_3$–$Pb(Fe_{1/5}Nb_{1/5}Sb_{3/5})O_3$, and $PbZrO_3$–$Pb(Mg_{1/3}Nb_{2/3})O_3$, which find tremendous applications in the electroceramic industries [13–15]. In all these applications, the stoichiometry and homogeneity of materials are known to be the important factor for ensuring the performance of devices [14, 15]. This is especially important in PZT compositions in which the useful properties depend significantly on Zr/Ti ratio [1, 14, 16]. Over decades, tremendous amount of work has been dedicated to the processing of PZT with various preparation routes, one of which is a modified mixed oxide route [1, 17, 18]. In this route, the PZT is prepared by mixing precursor PZ with $PbTiO_3$ or PbO and TiO_2 powders [1, 19, 20]. This preparation route, as well as the B-site cations route, offers advantages in producing PZT with more controllable Zr/Ti ratio and desirable properties at lower sintering temperature without using excess PbO typically practiced in a more conventional mixed-oxide method [17, 21, 22]. The resulting PZT is, however, found to show variation in properties, probably caused in part by the stoichiometry of PZ precursor powders. In addition, earlier work by Reaney et al. [23] reported that impure PZ specimen showed significantly inferior electrical properties as well as unclear TEM results in the antiferroelectric–ferroelectric (AFE-FE) phase boundary as a result of unreacted ZrO_2 phases. These reasons outlined have

W. Chaisan · O. Khamman · R. Yimnirun ·
S. Ananta (✉)
Department of Physics, Faculty of Science, Chiang Mai University, Chiang Mai 50200, Thailand
e-mail: Supon@chiangmai.ac.th

clearly indicated from both practical and fundamental viewpoints needs to obtain stoichiometric and better homogeneity PZ. To do such, different preparative methods have been introduced, such as chemical co-precipitation [24], sol–gel [25], precipitation of molecular precursors [26], citrate combustion [27], hydrothermal [28] and microemulsion method [29]. All these techniques are aimed at reducing the temperature of preparation of the compound even though they are more involved and complicated in approach than the solid-state reaction method. Moreover, high purity PZ powders are still not available in mass quantity and also expensive. So far, only limited attempts have been made to improve the yield of $PbZrO_3$ by optimizing calcination conditions [30–32]. The effects of applied dwell time and heating/cooling rates have not yet been studied extensively. Therefore, it is our interest to explore a simple mixed oxide synthetic route for the production of PZ powders. The effect of calcination conditions on the development of phase, morphology and particle size of lead zirconate powders is investigated in this connection. The potential of a vibro-milling technique as a significant time-saving method to obtain single-phase lead zirconate powders, at low temperature and with small particles is also examined.

Experimental procedure

The starting materials were commercially available lead oxide, PbO (JCPDS file number 77-1971) and zirconium oxide, ZrO_2 (JCPDS file number 37-1484) (Fluka, >99% purity). The two oxide powders exhibited an average particle size in the range of 3.0–5.0 µm. $PbZrO_3$ powders were synthesized by the solid-state reaction of thoroughly ground mixtures of PbO and ZrO_2 powders that were milled in the required stoichiometric ratio. Instead of employing a ball-milling procedure (ZrO_2 media under ethanol for 24 h [30] or under a mixture of cyclohexane and deionized water for 12 h [31]), use was made of a McCrone vibro-milling technique [22, 32, 33]. In order to combine mixing capacity with a significant time saving, the milling operation was carried out for 0.5 h with corundum cylindrical media in isopropyl alcohol (instead of 8 h with zirconia media [32]). After drying at 120 °C for 2 h, the reaction of the uncalcined powders taking place during heat treatment was investigated by themogravimetric and differential thermal analysis (TG-DTA, Shimadzu), using a heating rate of 10°C/min in air from room temperature up to 1000 °C. Based on the TG-DTA results, the mixture was calcined at various conditions, i.e. temperatures ranging from 700 to 900 °C, dwell times ranging from 1 to 5 h and heating/cooling rates ranging from 1 to 20 °C/min, in closed alumina crucible, in order to investigate the formation of lead zirconate.

Calcined powders were subsequently examined by room temperature X-ray diffraction (XRD; Siemens-D500 diffractometer), using Ni-filtered CuK_α radiation to identify the phases formed and optimum calcination conditions for the formation of $PbZrO_3$ powders. Crystallite sizes and lattice parameters in the calcined powders were estimated from XRD data [34, 35]. Powder morphologies and particle sizes were directly imaged, using scanning electron microscopy (SEM; JEOL JSM-840A).

Results and discussion

The TG-DTA simultaneous analysis of a powder mixed in the stoichiometric proportions of $PbZrO_3$ is displayed in Fig. 1. In the temperature range from room temperature to ~150 °C, the sample shows both exothermic and endothermic peaks in the DTA curve, in consistent with a slight drop in weight loss at the same temperature range. These observations can be attributed to the decomposition of the organic species (most likely polyethylene from the milling jar) from the milling process. [22, 33]. Corresponding to a large fall in sample weight (~4.5%), the other exotherm and endotherm are observed within 300–450 °C temperature range in the DTA curve. However, it is to be noted that there is no obvious interpretation of these peaks, although it is likely to correspond to a phase transformation of ZrO_2 precursor alloyed with PbO precursor reported by a number of workers [35–38]. In general, it is well established that there are a number of polymorphic forms of PbO and ZrO_2 stable at different temperatures and pressures [35, 37]. However, in this
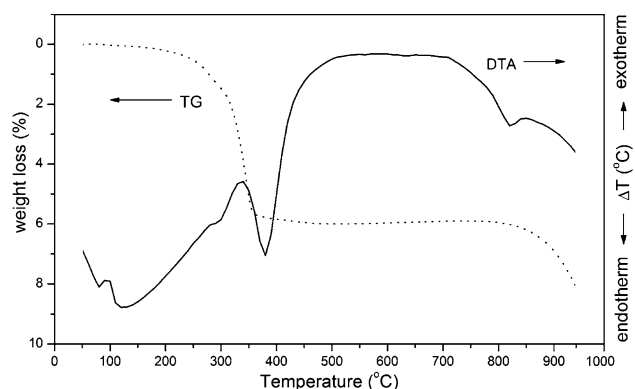
**Fig. 1** TG-DTA curves for the mixture of PbO–ZrO_2 powders

work, the possibility of these phase transformations has not been investigated, since the overriding objective is to synthesize single phase $PbZrO_3$, irrespective of the polymorph in which it is stabilized.

Increasing the temperature up to ~1000 °C, the solid-state reaction occurred between PbO and ZrO_2 [29–32]. The broad exotherm from 500 to 700 °C in the DTA curve represents that reaction, which is supported by a gradual decrease in sample weight over the same temperature range. Finally, a significantly drop in weight loss is also observed above 800 °C, that is associated with the DTA peaks at the same temperature range and may be attributed to the PbO volatilization commonly found in the lead-based perovskite systems [22, 33, 39]. These data were used together with those from literature [30–32] to assign the range of calcination temperatures for XRD investigation between 700 and 900 °C.

Therefore, to investigate the effect of calcination temperature on the phase development, the mixed powders were calcined for 2 h in air at various temperatures, up to 900 °C, followed by phase analysis using XRD. As shown in Fig. 2, for the uncalcined powder, only X-ray peaks of precursors PbO (▼) and ZrO_2 (●), which could be matched with JCPDS file numbers 77-1971 [40] and 37-1484 [41], respectively, are present, indicating that no reaction had yet been triggered during the milling process. It is seen that fine $PbZrO_3$ crystallites (*) were developed in the powder at a calcination temperature as low as 750°C, accompanying with PbO and ZrO_2 as separated phases. This observation agrees well with those derived from the

TG-DTA results and other workers [31, 38]. As the temperature increased to 800 °C, the intensity of the perovskite-like $PbZrO_3$ peaks was further enhanced and became the predominant phase. Upon calcination at 850 °C, an essentially monophasic of $PbZrO_3$ phase is obtained. This PZ phase was indexable according to an orthorhombic perovskite-type structure with lattice parameters a = 823.1 pm, b = 1177 pm and c = 588.1 pm, space group $P2cb$ (no. 32), in consistent with JCPDS file numbers 35-739 [42] and other investigators [24, 30, 43]. This study also shows that crystalline orthorhombic PZ is the only detectable phase in the powder, after calcination in the range 850–900 °C.

Having established the optimum calcination temperature, dwell times ranging from 1 to 5 h with constant heating/cooling rates of 5°C/min were applied at 850 and 800 °C, as shown in Figs. 3 and 4, respectively. From Fig. 3, it can be seen that the single phase of $PbZrO_3$ (yield of 100% within the limitations of the XRD technique) was found to be possible in all powders calcined at 850 °C with dwell time ranging from 1 to 5 h. This is probably due to the effectiveness of vibro-milling and a carefully optimized reaction. However, in the work reported here, it is to be noted that single-phase of $PbZrO_3$ powders was also successfully obtained for a calcination temperature of 800 °C with dwell time of 3 h or more applied (Fig. 4). This was apparently a consequence of the enhancement in crystallinity of the $PbZrO_3$ phase with increasing dwell time. The appearance of PbO phase indicated that full crystallization has not occurred at relatively shorter calcination times. The observation
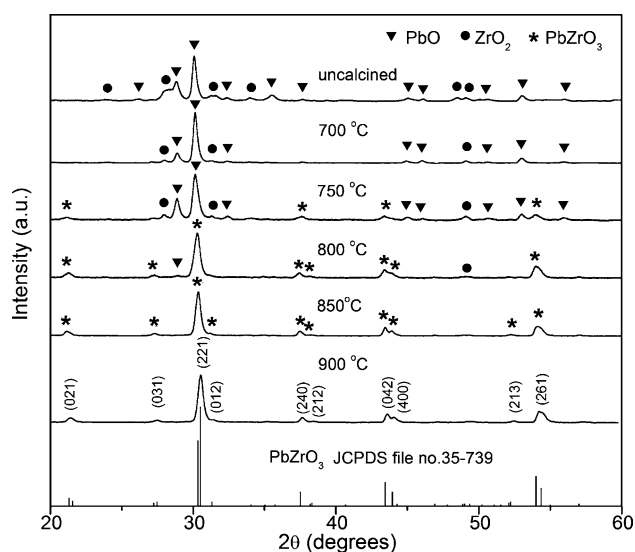
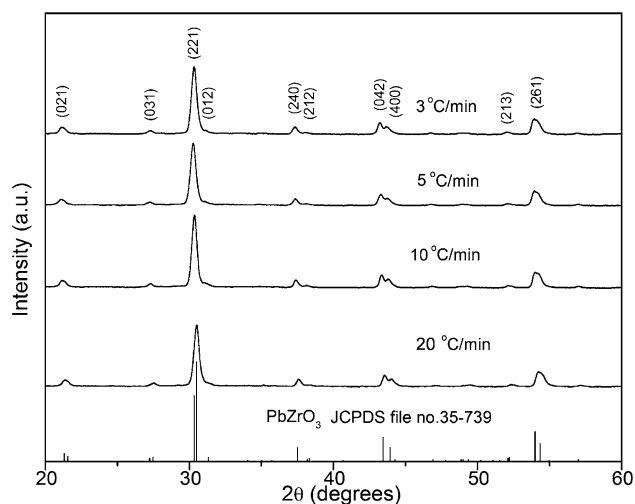**Fig. 2** XRD patterns of PZ powder calcined at various temperatures for 1 h with heating/cooling rates of 10°C/min
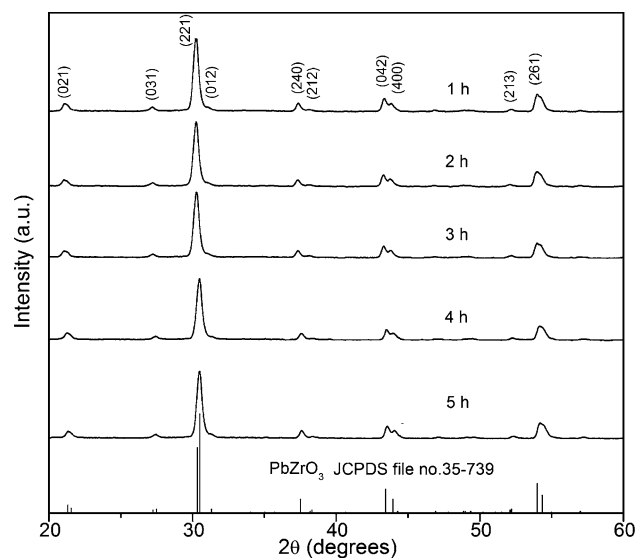
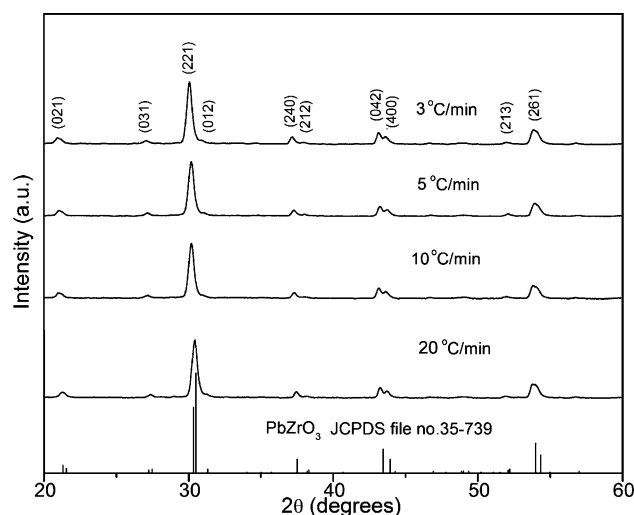**Fig. 3** XRD patterns of PZ powder calcined at 850 °C with heating/cooling ratesof 10 °C/min for various dwell times
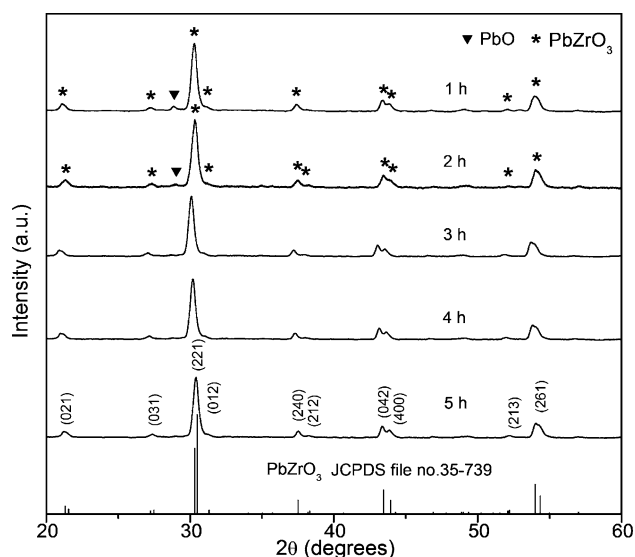
Fig. 4 XRD patterns of PZ powder calcined at 800 °C with heating/cooling rates of 10 °C/min for various dwell times

Fig. 6 XRD patterns of PZ powder calcined at 850 °C for 1 h with various heating/cooling rates

that the dwell time effect may also play an important role in obtaining a single-phase perovskite product is also consistent with other similar systems [33, 39, 44].

Apart from the calcination temperature and dwell time, the effect of heating/cooling rates on the formation behavior of $PbZrO_3$ was also investigated. Various heating/cooling rates ranging from 1 to 20 °C/min were selected for calcination conditions of 800 °C for 3 h (Fig. 5) and 850 °C for 1 h (Fig. 6). In this connection, it is shown that the yield of $PbZrO_3$ phase was not depending on heating/cooling rates, indicating that fast heating/cooling rates can lead to full crystallization of $PbZrO_3$ phase without time for the formation of minor

phase or lead vaporization. The observation that faster heating/cooling rates are required for lead-based ferroelectrics is also consistent with other researchers [39, 45, 46]. It should be once again emphasized that these results clearly indicate effects of heating/cooling rates on the phase formation behavior of PZ powders. These parameters are very crucial for Pb-based compounds [22, 47]. Usually, heating/cooling rates and dwell time show marked influences on phase formation behavior of other Pb-based compounds, such as PZT. It is of interest to observe that in PZ powders the heating/cooling rates do not show any effects on the behavior, while the dwell time only shows the effects on the particle agglomeration.

Based on the TG-DTA and XRD data, it may be concluded that, over a wide range of calcination conditions, single phase $PbZrO_3$ cannot be straightforwardly formed via a solid-state mixed oxide synthetic route, unless carefully designed calcination condition was performed. It is well documented that powders prepared by a conventional mixed oxide method have spatial fluctuations in their compositions. The extent of the fluctuation depends on the characteristics of the starting powders as well as the processing schedules [22, 33, 39]. The experimental work carried out here suggests that the optimal calcination conditions for single-phase $PbZrO_3$ (with impurities undetected by XRD technique) is 800 °C for 3 h or 850 °C for 1 h, with heating/cooling rates of 20 °C/min, which is closed to that of Puchmark et al. [30] (775 °C for 3 h with heating/cooling rates of 5 °C/min) but with significantly faster heating/cooling rates. Moreover, the formation temperature and/or dwell time for the production of

Fig. 5 XRD patterns of PZ powder calcined at 800 °C for 3 h with various heating/cooling rates

PbZrO$_3$ powders observed in this work are also lower than those reported by Fang et al. [31] (900 °C for 1 h) and Lanagan et al. [32] (900 °C for 8 h).

Finally, the morphological changes in the PbZrO$_3$ powders formed by a mixed oxide are illustrated in Fig. 7 as a function of calcination temperatures, dwell times and heating/cooling rates, respectively. The influence of calcination conditions on particle size is given in Table 1. These particle size data were directly estimated from SEM micrographs. Even though these data are not precisely determined, they were shown to provide estimated comparison between different calcination conditions and to form a basis for other more detailed studies with use of a combination between TEM and particle size distribution analyzer. After calcinations at 800 to 900°C, the powders seem to have similar morphology. In general, the particles are agglomerated and irregular in shape, with a substantial variation in particle size, particularly in samples calcined at higher temperatures or for longer dwell times. This observation is also similar to that of Mg$_4$Nb$_2$O$_9$ powders synthesized by Ananta [48]. The results indicate that averaged particle size and degree of agglomeration tend to increase with calcination temperature and dwell time (Table 1). However, the smallest particle size (estimated from SEM micrographs to be ~250 nm) and the morphology of the calcined powders are about the same. It is also of interest to point out that no evidence has been obtained for the existence of the cubic or spherical shape morphology as that of the hydrothermally derived PbZrO$_3$ powders [28, 49].

Conclusions

The methodology presented in this work provides a simple method for preparing perovskite PbZrO$_3$ powders via a solid-state mixed oxide synthetic route. By using optimal calcination conditions of 800 °C for 3 h or 850 °C for 1 h, with heating/cooling rates of 20 °C/min, the reproducible, low cost and fast process involving vibro-milling can provide high-purity perovskite PbZrO$_3$ powders with particle size ranging from 200–500 nm from inexpensive commercially available raw materials. The resulting PbZrO$_3$ powders consist of variety of agglomerated particle sizes, depending on calcination conditions. Finally, it should be emphasized that this work presents for the first time the effects of calcination conditions on the phase formation behavior of the PZ powders. These parameters clearly show significant influences on the processing of even simple binary system as PZ, and there is no doubt that they will show even more effects on other complicated materials such as PZT, PMN, PZN, PIN, and PMN-PT. The results on those systems are being produced and will be presented in future publications.

Fig. 7 SEM micrographs of the PZ powders calcined at (**a**) 850 °C/1h, (**b**) 850 °C/2 h, (**c**) 900 °C/2 h, with heating/cooling rates of 10 °C/min and (**d**) 850 °C/1 h with heating/cooling rates of 20 °C/min
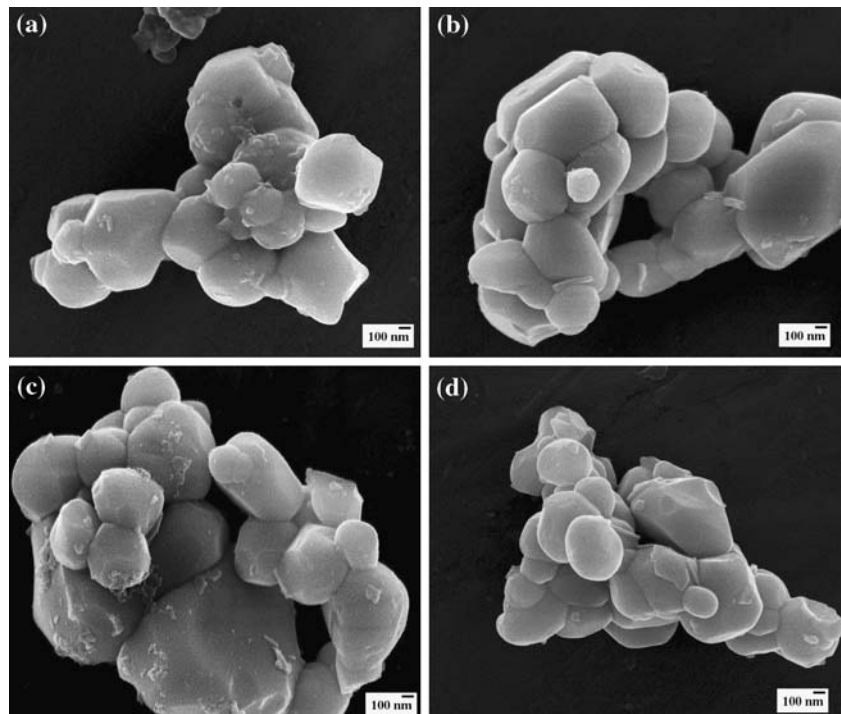
Table 1 Particle size range of $PbZrO_3$ powders calcined at various conditions

Temperature (°C)	Dwell time(h)	Heating/cooling rates(°C/min)	Particle size range (mean)*(μm)
800	3	3	0.35–0.60 (0.41)
800	3	5	0.15–1.00 (0.52)
850	1	3	0.30–1.00 (0.44)
850	1	5	0.30–0.80 (0.59)
850	1	10	0.25–0.70 (0.54)
850	1	20	0.30–0.80 (0.51)
850	2	10	0.25–1.20 (0.64)
900	2	10	0.35–1.50 (0.77)

*The estimated precision of the particle size is ±10%

References

1. Jaffe B, Cook WJ, Jaffe H (1971) Piezoelectric ceramics. Academic Press, London
2. Jona F, Shirane G (1993) Ferroelectric crystals. Dover Publications, New York
3. Sawaguchi E, Maniwa H,Hoshino S (1951) Phys Rev 83:1078
4. Shirane G, Sawaguchi E, Takagi Y (1951) Phys Rev 84:476
5. Sawaguchi E, Kittaka K (1952) J Phys Soc Jpn 7:336
6. Tennery VJ (1966) J Am Ceram Soc 49:483
7. Scott BA, Burns G (1972) J Am Ceram Soc 55:331
8. Shirane G, Hoshino S (1954) Acta Crystallogr **7**:203
9. Pokharel BP, Pandey D (1999) J Appl Phys 86:3327
10. Bongarn T, Rujijanagul G, Milne SJ (2005) Mater Lett 59:1200
11. Whatmore RW (1976) Ph.D. Thesis, Genville and Cauis College, Cambridge
12. Singh K (1989) Ferroelectrics 94:433
13. Haertling GH (1999) J Am Ceram Soc 82:797
14. Moulson AJ, Herbert JM (2003) Electroceramics, 2nd edn. Wiley, New York
15. Uchino K (1998) Piezoelectrics and ultrasonic applications. Kluwer, Deventer
16. Kakegawa K, Mohri J, Takahashi T, Yamamura H, Shirasaki S (1977) Solid State Commun 24:769
17. Kingon AI, Clark JB (1983) J Am Ceram Soc 66:253
18. Matsuo Y, Sasaki H (1965) J Am Ceram Soc 48:289
19. Babushkin O, Lindback T, Lue JC, Leblais JYM (1996) J Eur Ceram Soc 16:1293
20. Hanky DL, Biggers JV (1951) J Am Ceram Soc 12:172
21. Garg A, Agrawal DC (1999) Mat Sci Eng B 56:46
22. Tipakontitikul R, Ananta S (2004) Mater Lett 58:449
23. Reaney IM, Glazounov A, Chu F, Bell A, Setter N (1997) Brit Ceram Trans 96:217
24. Oren EE, Taspinar E, Tas AC (1997) J Am Ceram Soc 80:2714
25. Ibrahim DM, Hennicke HW (1981) Trans J Br Ceram Soc 80:18
26. Deshpande AS, Khollam YB, Patil AJ, Deshpande SB, Potdar HS, Date SK (2001) Mater Lett 51:161
27. Rao YS, Sunandana CS (1992) J Mater Sci Lett 11:595
28. Choi JY, Kim CH, Kim DK (1998) J Am Ceram Soc 81:1353
29. Fang J, Wang J, Ng SC, Gan LM, Quek CH, Chew CH (1998) Mater Lett 36:179
30. Puchmark C, Rujijanagul G, Jiansirisomboon S, Tunkasiri T (2004) Ferroelectric Lett 31:1
31. Fang J, Wang J, Ng SC, Gan LM, Chew CH (1998) Ceram Inter 24:507
32. Lanagan MT, Kim JH, Jang S, Newnham RE (1988) J Am Ceram Soc 71:311
33. Ananta S, Thomas NW (1999) J Eur Ceram Soc 19:155
34. Klug H, Alexander LE (1974) X-ray diffraction procedures for polycrystalline and amorphous materials, 2nd edn. Wiley, New York
35. Aoyama T, Kurata N, Hirota K, Yamaguchi O (1995) J Am Ceram Soc 78:3163
36. Fushimi S, Ikeda T (1967) J Am Ceram Soc 50:129
37. Lee WE, Rainforth WM (1994) Ceramic microstructures: Property control by processing. Chapman & Hall, London
38. Deyneka TG, Vouk EA, Ishchuk VM, Ramakaeva RF, Volkova GK, Konstantinova TE (2004) Funct Mater 11:44
39. Udomporn A, Ananta S (2004) Mater Lett 58:1154
40. JCPDS-ICDD Card No. 77-1971 (2002) International Centre for Diffraction Data, Newtown Square, PA
41. JCPDS-ICDD Card No. 37-1484 (2002) International Centre for Diffraction Data, Newtown Square, PA
42. JCPDS-ICDD Card No. 35-739 (2002) International Centre for Diffraction Data, Newtown Square, PA, 2002
43. Tani T, Li JF, Viehland D, Payne DA (1994) J Appl Phys 75:3017
44. Ananta S, Brydson R, Thomas NW (2000) J Eur Ceram Soc 20:2315
45. Ryu J, Choi JJ, Kim HE (2001) J Am Ceram Soc 84:902
46. Baumgartner CE (1988) J Am Ceram Soc 71:C-350
47. Udomporn A, Pengpat K, Ananta S (2004) J Eur Ceram Soc 24:185
48. Ananta S (2004) Mater Lett 58:2530
49. Kim HK (1993) Thesis MS, Seoul National University, Seoul, Korea